Journal of Structural Chemistry. Vol. 51, No. 3, pp. 482-490, 2010

EFFECT OF HYDROGEN BRIDGE GEOMETRY ON THE VIBRATIONAL SPECTRA OF WATER: THREE-PARAMETER POTENTIAL OF H BOND

Yu. Ya. Efimov

UDC 532.74

The ability of water molecules to form a three-dimensional network of hydrogen bonds basically determines both the intrinsic structure and unique properties of this liquid and also a character of interactions with other molecules. However, the dependence of the H bond energy on the geometry of its hydrogen bridge, namely on the $R_{O...O}$ length and non-linearity, is unknown, i.e. the deviations of O–H group directions and the lone pair forming this bond from optimum ones (angles φ = H–O…O and χ = –O…O correspondingly). Even in computer simulation methods, the contribution of H bonds to the total interaction potential is not separated; that does not allow one to define unequivocally these bonds in a model and to analyze quantitatively the features of their networks. The purpose of this work is to fill in this gap by expressing the energy E through geometric parameters (R, φ, χ). The obtained solution quality is proved by an agreement between the distributions of OH vibrational frequencies (which are very sensitive to the H bond strength) calculated with its help and the shape of experimental spectra in a wide temperature range. Based on this, the distributions of H bond energies $P(E, T)$ and of their bend angles $P(\varphi, T)$ and $P(\chi, T)$ are also calculated. It is shown that the main contribution to spectra is made by the shortest bonds with their lengths close to a minimum of the potential $E(R)$. Thus, the low-frequency slope of a band corresponds to slightly bent H bonds, while the central part relates to also short but sufficiently nonlinear H bonds. LongH bonds are responsible for only well known high-frequency Walrafen's wing near 3620 cm^{-1}. Moreover, these weak bonds are very strongly bent.

Keywords: liquid water, continuum model, hydrogen bond, fluctuation theory, geometry, potential, vibrational spectra.

INTRODUCTION

The continuum model [1] assumes discrete species (monomers, dimers, etc.) to be absent in liquid water. Its structure is based on a three-dimensional network of H bonds that are different in the geometric parameters of O–H…O hydrogen bridges and in binding energies E. The frequency of the maxima of broad bands of O–H vibrations in various systems (not only aqueous) has been long known to correlate with the average energy of H bonds in a system [2]. It appears to be also true for each individual hydrogen bond. Thus, the wide spectral band is represented by a set of narrow lines. The frequency of each of them ν_{OH} unambiguously determines the energy E of the H bond in which this O–H group is involved

Institute of Chemical Kinetics and Combustion, Siberian Division, Russian Academy of Sciences, Novosibirsk; efimov@kinetics.nsc.ru. Translated from *Zhurnal Strukturnoi Khimii*, Vol. 51, No. 3, pp. 501-508, May-June, 2010. Original article submitted June 27, 2009.

 0022-4766/10/5103-0482

[3]. The form of the statistical distribution of these frequencies and even its very characteristic temperature evolution is perfectly described by the simple Boltzmann formula [4]

$$P(\nu,T)=Q^{-1}(T)W(\nu)\exp[-E(\nu)/(kT)]. \quad (1)$$

Here $Q(T)$ is the statistical integral (statistical sum) normalizing the distribution $P(\nu, T)$; $W(\nu)$ is the degeneracy of states corresponding to the frequency ν i.e. a fraction of all geometric configurations of hydrogen bridges able to generate the frequency ν. The actual occurrence of these configurations at a temperature T is defined by the exponent $\exp[-E(\nu)/(kT)]$. A comparison of the experimental spectra of O–H vibrations of water for several temperatures has allowed us to find the interrelation of E and W with the frequency ν_{OH} in the explicit form, and both functions $E(\nu)$ and $W(\nu)$ in (1) proved to be indeed independent of the temperature. Consequently, infrared and Raman spectra of HOD molecules in D_2O that are essentially different in their form have been quantitatively described for the first time within the limits of the uniform theory at constant density in all studied range of temperatures [5, 6]. It is a forcible argument in favor of the continuum model of the water structure.

A successful theoretical description of the shape and temperature evolution of the statistical distribution of frequencies ν_{OH} allows us to assume the probability of occurrence of the hydrogen bridge with the geometry (R, φ, χ) to be also described using a similar expression

$$\mathrm{P}(R,\varphi,\chi,T)=Q^{-1}(T)W(R,\varphi,\chi)\ \exp[-E(R,\varphi,\chi)/(kT)]. \quad (2)$$

However, if in [5, 6] the degeneracy of H bonds $W(\nu)$, which generate the frequency ν_{OH} in a spectrum, was a "thing in itself" and was obtained from experiments, then in (2), its analogue can be defined as a volume element in the space of configurations, $W(R, \varphi, \chi) = 4\pi R^2\sin(\varphi)\sin(\chi)$ [7]. It determines the purely geometric probability for a proton donor OH group of one water molecule to meet a proton acceptor O atom of another molecule at a distance $R_{O...O}$ if the deviation angles of the OH group direction and the oxygen atom lone pair from an ideal (linear) configuration of a hydrogen bridge are φ and χ respectively. The degeneracy of a particular configuration of a hydrogen bridge being thus defined certainly does not depend on the H bond energy. The latter determines the total probability of the occurrence of such a configuration at a temperature T by the factor $\exp[-E(R, \varphi, \chi)/(kT)]$, as well as in formula (1). Therefore the problem is reduced to finding the dependence $E(R, \varphi, \chi)$ that would allow the computer reproduction of the form and temperature evolution of real spectra by an exhaustive search of every possible sets of three parameters (R, φ, χ) with the weight $W(R, \varphi, \chi)\exp[-E(R, \varphi, \chi)/(kT)]$ with regard to the known functions $W(\nu)$ and $E(\nu)$. The strict solution has been found only for one-parameter potentials $E(R)$ or $E(\varphi)$, in the terms of which this problem was originally formulated [8]. Already in the case of two parameters (R, φ) [7], it becomes an incorrect reverse problem of search of $\nu_{OH}(R, \varphi)$, which includes the solution of the integral equation of the form

$$\iint\limits_{(R,\varphi):\nu\le\nu_{OH}} W(R,\varphi)dRd\varphi = \int_0^{\nu_{OH}} W(\nu)d\nu. \quad (3)$$

Using reasonable simplifications, in [7] we have managed to obtain the required dependence for both $E(R, \varphi)$ and the alternative potential $E(\varphi, \chi)$. The given work completes a series [7, 8] by finding a solution for the total problem with three-parameter potential of hydrogen bond.

CALCULATION OF THE THREE-PARAMETER POTENTIAL

As in [7], the effect of the hydrogen bond length R and its both bend angles φ and χ on a low-frequency shift of the frequency ν_{OH} relative to its non-perturbed (monomeric) value $\nu_u = 3707\ \mathrm{cm}^{-1}$ we consider as multiplicative

$$(\nu_u-\nu_{OH})=\Phi(R)\cdot F(\varphi)\cdot f(\chi), \quad (4)$$

The radial dependence $\Phi(R)$ is borrowed from the empirical correlation [9], where R is expressed in angströms and frequencies in reciprocal centimeters in (4)

$$\Phi(R)=2.222\cdot 10^7\exp(-3.925R). \quad (5)$$

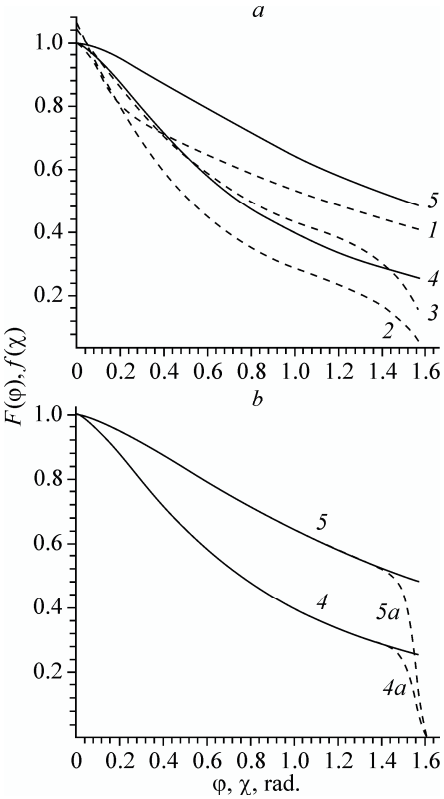

Fig. 1. Angular factors of H bond weakening: F (φ) and $f(\chi)$ are the multipliers in formula (4). *a*) Dashed lines are borrowed from [7] as $\sqrt{F_1}(\varphi)$ for the dependence ν(*R*, φ) (curve *1*) and as $F(\varphi)$ and $f(\chi)$ for the dependence ν(φ, χ) with neglected effect of *R* (curves *2* and *3*). Solid curves *4* and *5* are calculated by formulas (6) with $n = 1.45$ and $\sigma = 0.75$; *b*) Curves *4* and *5* are taken from Fig. 1*a*; updated by expression (7), they are shown by dashed curves.

Dependences $F(\varphi)$ and $f(\chi)$ should be the functions that monotonically decrease from unit to zero with increasing corresponding angle from zero (linear hydrogen bond) up to the limiting values φ_{lim} and χ_{lim}. This makes the H bond break and form a new one. In particular, for linear H bonds in the liquid, formula (4) describes a decrease in the frequency shift with increasing bond length, as in crystals [10, 9]. A deviation of the O–H group direction and/or a lone pair from the linear geometry of a hydrogen bond results in further weakening of this bond and reduction of the corresponding frequency shift; thus, the ν_{OH} value monotonically approaches the vibrational frequency of the free OH group $\nu_u = 3707$ cm^{-1}.

Since it was impossible to find the strict solution ν(φ, χ) of the reverse problem already in the case of two-parameter potential [7], here we do not even try to solve a three-parameter analogue of integral equation (3). Instead, being guided by the form of the previously found angular dependences (Fig. 1*a*), we try to most simply set a form of their functional dependence with a minimum of parameters (two)

$$F(\varphi)=1/[1+(\varphi/\sigma)^n], \tag{6a}$$

$$f(\chi)=1/[1+(\chi/2\sigma)^n], \tag{6b}$$

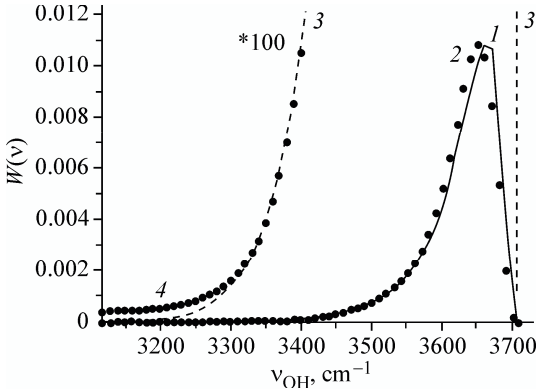

Fig. 2. Function of H bond configuration degeneracy that generates the frequency ν_{OH} in a spectrum: *1* our calculation (see the text), *2* $W(\nu)$ obtained from the experimental spectra, *3* and *4* the same curves multiplied by 100 for better visualization of the low frequencies region.

and then refine these parameters by solving **a direct** problem of expressing ν through (R, φ, χ) in (4) so that to reach the best agreement between the calculated function $W(\nu)$ and that known from spectroscopic experiments. The doubled width parameter 2σ for the angle χ in (6b) corresponds to a distinction between previously found (with neglected R) curves *2* (for φ) and *3* (for χ) in Fig. 1. Physically, this difference reflects the larger sensitivity of a hydrogen bond to the O–H group orientation than that of the lone pair. (One can easily notice that for $n = 2$ curves (6) represent Lorentzians.)

To calculate the function $W(\nu)$ for given n and σ we regularly searched about one million triplets of parameters (R, φ, χ) in the intervals $R_{min} \le R \le R_{lim}$, $0 \le \varphi, \chi \le \pi/2$. The shortest H bond with the length $R_{min} = 2.6857$ Å by formulas (4), (5) at $F(\varphi) = f(\chi) = 1$ (i.e. $\varphi = \chi = 0$) corresponds to the low-frequency end of the O–H vibrational spectrum, $\nu_{min} = 3120$ cm^{-1}; the limit angles of the H bond bend φ_{lim} and χ_{lim} are set equal to $\pi/2$ for simplicity. The value of the limiting length of a hydrogen bridge $R_{lim} \approx 3.1$ Å found in [7, 8] was refined in the calculations. For each triplet (R, φ, χ) we calculate the corresponding frequency ν_{OH} by formula (4), and the contribution of this triplet $\Delta W_i = R^2\sin(\varphi)\sin(\chi)$ to the total degeneracy of the states generating the frequency $\nu_{OH} = \nu_i \pm 5$ cm^{-1} is added to the respective element of the discrete array $W[\nu_i]$. Certainly, the contributions from all other triplets (R, φ, χ), whose calculated frequencies ν_{OH} belong to the ±5 cm^{-1} interval relative to the center of ith box ν_i, are added to the content of the same element of the array $W[\nu_i]$ in the course of calculations.

Simultaneously with $W(\nu)$ we calculate the statistical distributions of frequencies $P(\nu)$ and angles $P(\varphi)$ and $P(\chi)$ in the same threefold cycle of the program (over R, φ, and χ). For this purpose, the corresponding arrays (sequences of boxes) $P[\nu_i]$, $P[\varphi_i]$, $P[\chi_i]$ are also created and filled up with ΔW_i products multiplied to the energy probability of the occurrence of a given configuration at a temperature T, $\exp[-E(R, \varphi, \chi)/(kT)]$. The required hydrogen bond energy $E(R, \varphi, \chi)$ is calculated (in kJ/mol) from the obtained frequency ν_{OH} using the formula found in [11]

$$E(x) = -0.07x + 0.000104x^2 - 0.493\cdot10^{-6}x^3 + 0.1224\cdot10^{-8}x^4 - 0.828\cdot10^{-12}x^5;$$
$$x = 3707 - \nu_{OH}(\text{cm}^{-1}). \qquad (7)$$

Quite good agreement of the calculated function $W(\nu)$ (Fig. 2, lines) with that obtained in [11] based on the experimental spectra [12] (dots) is reached for $n = 1.45$, $\sigma = 0.75$ in formulas (6). In addition, the initial limiting H bond length R_{lim} should be reduced by 0.05 Å to 3.05Å. The corresponding curves $F(\varphi)$ and $f(\chi)$ are represented by solid lines in Fig. 1*a*. However, unlike curves *2* and *3* obtained in [7] without allowance for R, they do not vanish when φ and χ tend to the limiting values. Hence, the calculated distributions of angles $P(\varphi)$ and $P(\chi)$ also do not tend to zero near $\pi/2$. It is easy to

correct this defect: let us multiply the angular factors of H bond weakening (6) by the function that does not deform them in the basic area of values, but sharply decreases close to π/2

$$G(\alpha)=\exp[-(\alpha/\sigma_G)^m], \quad \alpha=\varphi \quad \text{and} \quad \chi, m=50, \quad \sigma_G=1.56. \tag{8}$$

The functions $F(\varphi)$ and $f(\chi)$ thus modified are shown in Fig. 1*b* by dashed curves *4a* and *5a* and are used in all further calculations.

RESULTS AND DISCUSSION

The dependence of the O–H vibrational frequency of water molecules ν_{OH} on the hydrogen bridge geometry (formula (4) with allowance for (5) and (6)) is represented in Fig. 3; its radial component (for $\varphi = \chi = 0$, i.e. for a linear H bond) is displayed by a solid line in Fig. 4. In view of (5), it is described by the formula

$$\nu_{OH}(R)=3707 - 2.222\cdot 10^7 \exp(-3.925R). \tag{9}$$

The H bond energy E as a function of its length R (obtained by substituting (9) into (7)) is also shown in Fig. 4 by a dashed line. One can see that both the frequency ν_{OH} and the energy by far do not reach their limiting values of 3707 cm^{-1} and 0 kJ/mol respectively for the maximum H bond length R_{lim} = 3.05 Å when this H-bond breaks, as would be for a dimer in the gas phase. In dense liquid water, a weak H bond can be broken at much shorter distances, and the released O–H group switches to a more successfully located neighbor. In the absence of unfavorable long H bonds, all high-frequency wing of a spectrum at $\nu_{OH} > 3550$ cm^{-1} is provided by strongly bent hydrogen bonds (Fig. 3) with their energies exceeding –9 kJ/mol (Fig. 4).

The statistical frequency distributions calculated for three temperatures from 10°C to 200°C are shown in Fig. 5*a* by solid lines along with those obtained in [11] from the experimental infrared spectra [12]. The temperature evolution of distributions $P(\nu, T)$ obtained from Raman spectra is almost the same [5]. We believe the achieved agreement to be quite good, in view of a non ordinary character of the change in spectral shapes. Fig. 5*b* shows the calculated distributions of angles $P(\varphi)$ and $P(\chi)$, and Fig. 5*c* presents the H bond energy distributions at the same temperatures.

All four calculated properties display more or less expressed bimodal behavior: the presence of two regions of frequencies, bend angles, and hydrogen bond energies. This fact, which has been found for the first time in the Raman spectra of HOD molecules, is used to justify the mixed (two-structural) model of liquid water. In some variants of this model, all O–H groups were divided into those participating in hydrogen bonds and free (monomeric) ones; a temperature transformation

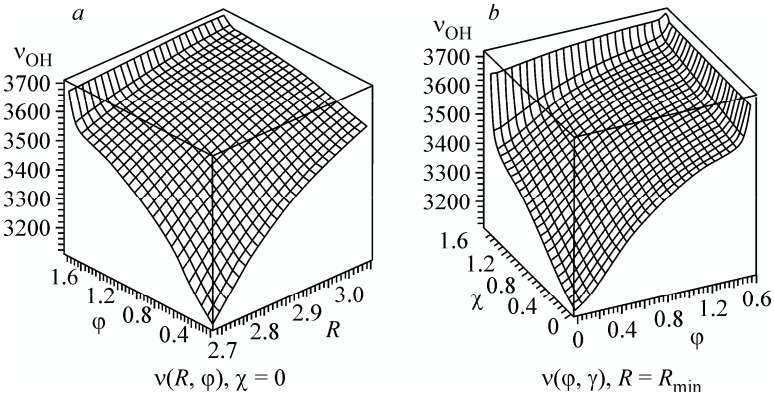

Fig. 3. Dependence of the O–H group vibrational frequency ν_{OH} of a water molecule on the hydrogen bridge geometry: its length $R_{O...O}$ and the angle φ at $\chi = 0$ (*a*) and on both angles φ and χ at $R_{O...O} = R_{min}$ (*b*). Calculations are performed by formula (4) with allowance for (5)-(8).

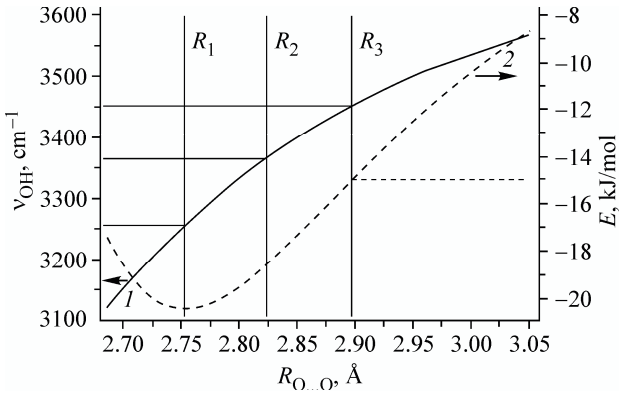

Fig. 4. Dependence of the O–H vibrational frequency calculated by formula (9) (solid curve, the left axis of ordinates) and the linear hydrogen bond energy (formula (7) with allowance for (9): dashed curve, the right axis of ordinates) on this bond length $R_{O...O}$ for $\varphi = \chi = 0$.

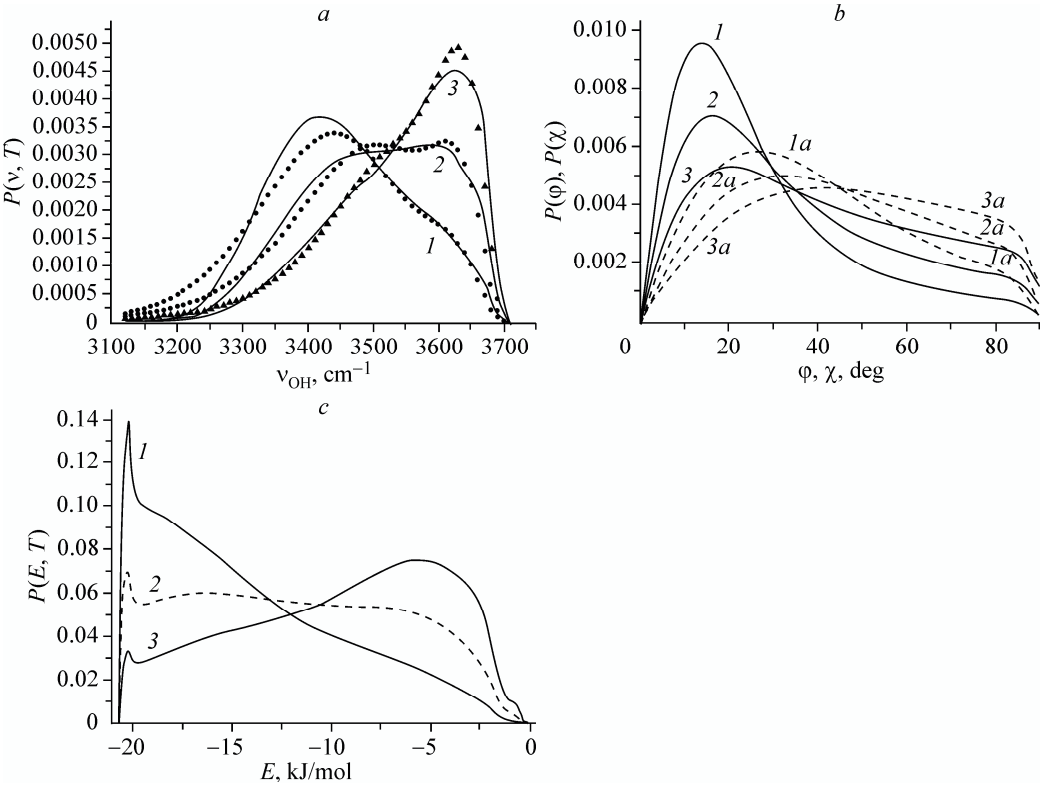

Fig. 5. Principal calculation results: temperature dependence of the O–H vibrational frequency distributions (*a*), bend angles of the hydrogen bridge φ and χ (*b*) and H bond energies (*c*) for temperatures: 10°C (curves *1*), 90°C (curves *2*) and 200°C (curves *3*). Lines: calculation, dots: experiment; solid: $P(\chi, T)$, dashed with a symbol "*a*" are $P(\chi, T)$.

of the spectral contour was explained by breakage of H bonds, i.e. a swap between these two types with the fixed properties. However, in this interpretation the vibrational band of free O–H groups should be much narrower and have a higher frequency; the band of H bonded O–H groups should not shift, but only decrease in intensity with temperature growth, according to all spectroscopic experience. Our calculations present a serious argument in favor of the continuum model of water because they are initially based on **continuous** statistical distributions of geometric parameters of hydrogen bridges

with **the monotonic** law of the temperature dependence of their shape. There is no place for discrete types of O–H groups or water molecules therein.

Figure 5*b* shows that the distributions $P(\varphi)$ and $P(\chi)$ become wider with increasing temperature, and their maxima shift to larger angles. The fraction of strongly bent hydrogen bonds also grows. All noted is much more strongly expressed for the deviation angles of a lone pair from the optimum geometry (dashed curves *1a-3a*) rather than for O–H groups (solid curves *1-3*). It reflects a sharper dependence of the H bond energy on the O–H group orientation.

For low temperatures strong ice-like hydrogen bonds with the energy of about 20 kJ/mol prevail in water; the fraction of weaker bonds monotonically decreases at E tending to zero (curve *1* in Fig. 5*c)*. At 200°C the situation changes to the opposite one and weak H bonds with the energy ≈6 kJ/mol become dominant (curve *3*). It is interesting that at 100°C all energies from 6 kJ/mol to 20 kJ/mol are almost equiprobable (curve *2* is calculated for $T = 90$°C where the experimental spectra are available, Fig. 5*a*). A sharp maximum in the distribution $P(E)$ and its breakage at –21 kJ/mol is hardly important. This breakage is caused by the absence of energies lower than –21 kJ/mol in the used potential (Fig. 4), and the unequivocal dependence $E(\nu)$ in (7) formally leads to $P(E)$ tending to infinity at E_{min} in view of $P(E) = P(\nu)/|\partial E/\partial\nu|$, as the derivative $|\partial E/\partial\nu|$ vanishes at this point. However, the function $P(E)$ does not diverge, which is also confirmed by our calculation with discrete intervals for E. It is not excluded that the true hydrogen bond energy $E_H(\nu)$ as the attraction energy will also continue to decrease in the region left to the minimum with further decreasing frequency. The minimum in the total $E(\nu)$ is caused by increasing repulsion energy $E_a(R_{O...O})$ between two oxygen atoms, probably, when they come too close (i.e. closer than in ice) in dense microregions of a liquid. This interaction does not change the frequency ν_{OH} that still correlates with $E_H(\nu)$, but its energy $E_a(R)$ as the summand affects a probability of the occurrence of a given configuration in the exponent of formulas (1) and (2). Thus, no peak will appear in the left wing of distributions $P(E_H)$.

Interesting information can be obtained by calculating the distributions presented in Fig. 5 for short and long hydrogen bonds separately. In the first group, we consider H bonds close to the energy minimum with lengths less than $R_2 =$ 2.823Å (Fig. 4). They are marked by a symbol *a* in Fig. 6. The second group contains all the rest with $R_{O...O} > R_2$, which are marked by a symbol *b*. Calculations are made for two temperatures: $T_1 = 50$°C (curves *1*) and T_2=300°C (curves *2*). The second temperature is the maximum for which we still managed to find the experimental spectra of water in *the liquid* state in the literature, i.e. with the density $\rho \sim 1$ g/cm^3 [5].

Figure 6*a* shows that the main contribution to the spectral contour is made by shorter hydrogen bonds at both temperatures, though at 300°C the contribution of long bonds considerably grows. Thus, the energy advantage (the exponent in formulas (1) and (2)) for short bonds exceeds the greater degeneracy $W \sim R^2$ for long bonds. An essential distinction of these two groups consists in that the spectral contour corresponding to short bonds strongly shifts to high frequencies (curves 1*a* and 2*a*) with increasing temperature, whereas for long bonds it remains unchanged (curves 1*b* and 2*b*). The latter are responsible for the high-frequency shoulder in Raman spectra that underlies the two-structural models. Since they have the energy of only 3-4 kJ/mol (curves 1*b* and 2*b* in Fig. 6*d*) we conventionally relate them to a subclass of weak hydrogen bonds. Note that even for these temperatures the calculated total spectra (solid lines in Fig. 6*a*) agree well with experiments (dots).

A comparison of hydrogen bonds by degree of their nonlinearity (Fig. 6*b* and *c)* shows that short H bonds get an additional benefit against long ones due to smaller bending (curves 1*a* and 2*a* in comparison with 1*b* and 2*b*). At 300°C (curves 2*b*) the probability of meeting a long bond even grows with increasing bend. Thus, most weak hydrogen bonds in water are characterized not only by a long length, but also the great nonlinearity. Together, these two factors explain the extremely small energy of their greater part (curves *2* in Fig. 6*d*). At the same time, the wings of distributions $P(E)$ of long H bonds are extended to –17 kJ/mol, which makes their separation into the individual class based on the H bond strength criterion rather arbitrary.

We saw that for all temperatures reached in experiments the probability of the occurrence of a hydrogen bridge with the given geometry is mainly determined by its energy. However (it is purely speculative), when the temperature tends to infinity (i.e. all possible H bond energies become equiprobable), the degeneracy of states should prevail. And it is really so:

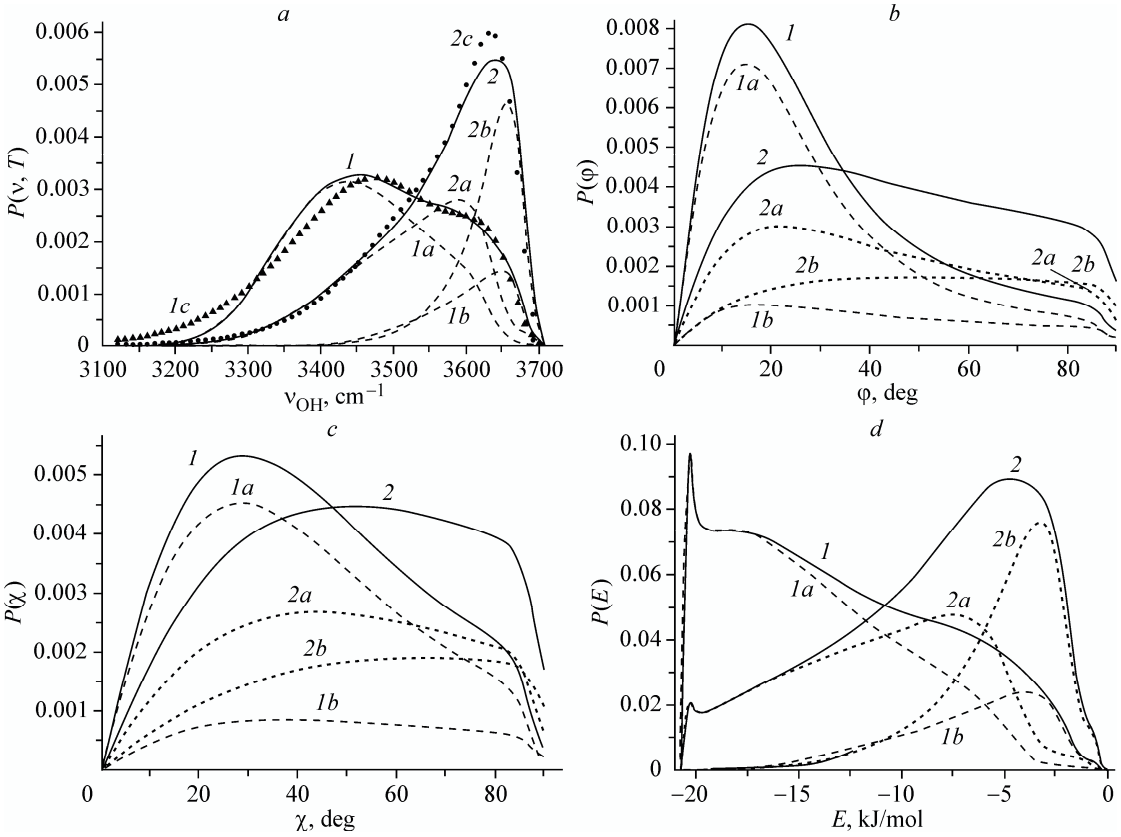

Fig. 6. Temperature dependence of the O–H vibrational frequency distributions (*a*), deviation angles of the O–H group φ (*b*) and a lone pair χ (*c*) relative to the linear H bond configuration and H bond energies (*d*) for temperatures 50°C (curves *1*) and 300°C (curves *2*). Dashed contours with symbols *a* and *b* correspond to short and long hydrogen bonds respectively (see the text); solid curves *1* and *2* are their sums. Dots 1*c* and 2*c* in Fig. 6*a* correspond to the experimental frequency distributions P (ν_{OH}, T).

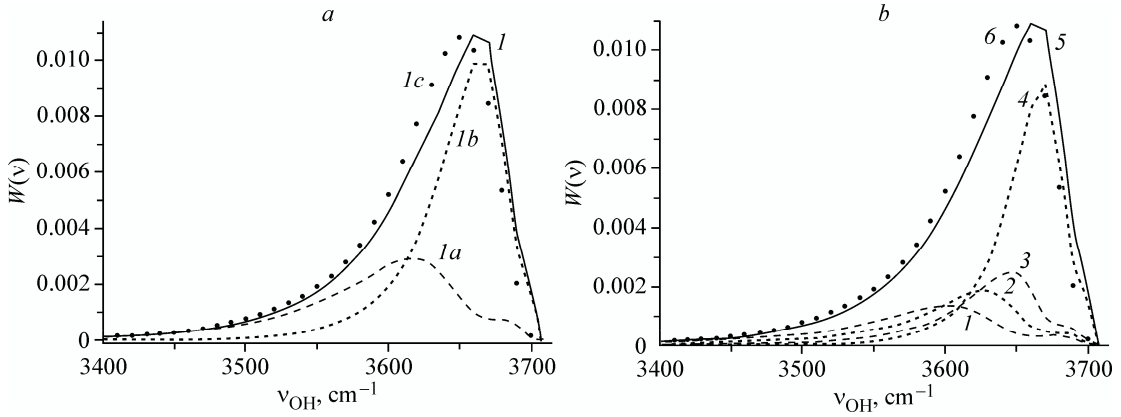

Fig. 7. Function of the degeneracy of configurations $W(\nu)$ calculated for groups of H bonds with different lengths: *a*) curve 1*a:* for $R_{O...O} < R_2$; curve 1*b:* for $R_{O...O} > R_2$ (Fig. 4). Solid line *1* is their sum. Dots 1*c:* $W(\nu)$ obtained from experimental spectra. *b*) The same as in Fig. 7*a* but with more detailed subdividing of the H bond lengths, see the interval limiters R_1, R_2, R_3 in Fig. 4. Curve *5* is the sum of contours *1-4*; dots *6* represent the experimental $W(\nu)$ (curve 1*c* in Fig. 7*a*).

the function $W(\nu)$ (into which the spectrum of frequencies $P(\nu)$ transforms at $T \to \infty$) calculated for two considered above groups of H bonds shows obvious prevalence of long H bonds (curve 1*b* against 1*a* in Fig. 7*a*). More detailed segmentation of a distance scale to four intervals (R_1, R_2, R_3 in Fg. 4) shows that H bonds with lengths above $R_3 = 2.892$ Å and energies

over –15 kJ/mol become dominant (Fig. 7). As one would expect, the longer the H bond, the larger its contribution to the degeneracy of states is (curves *1*-*3*).

CONCLUSIONS

The dependence of the O–H group vibrational frequency of a water molecule and the H bond energy, in which it is involved, on the main geometric parameters of the O–H…O hydrogen bridge is obtained in the analytical form. The distributions of stretching frequencies calculated based on them agree well with experimental ones in a wide temperature range. The distribution functions of bend angles of H bonds in liquid water are calculated. The role of a hydrogen bond length in the formation of these distributions is analyzed. These results can be used to analyze the properties of computer models of water, including the quantitative description of hydrogen bonds therein, and to reconstruct the vibrational spectrum corresponding to the given computer model.

This work was supported by RFBR grants Nos. 04-03-32560 and 07-03-32560.

REFERENCES

1. J. D. Bernal and R. H. Fowler, *J. Chem. Phys*., **1**, 515-548 (1933).
2. G. C. Pimentel and A. L. McClellan, in: *The Hydrogen Bond*, L. Pauling (ed.), Freeman, San Francisco (1960).
3. Yu. Ya. Efimov and Yu. I. Naberukhin, *Farad. Discuss. Chem. Soc*., **85**, 117-123 (1988).
4. A. P. Zhukovskii, *Zh. Strukt. Khim.*, **17**, 931/932 (1976).
5. Yu. Ya. Efimov and Yu. I. Naberukhin, *Mol. Phys*., **101**, 459-468 (2003).
6. Yu. Ya. Efimov and Yu. I. Naberukhin, *ibid*., **102**, 1407-1414 (2004).
7. Yu. Ya. Efimov, *J. Struct. Chem*., **50**, No. 4, 702-711 (2009).
8. Yu. Ya. Efimov, *ibid*., **49**, No. 2, 261-269 (2008).
9. Yu. Ya. Efimov, *ibid*., **32**, No. 6, 834-841 (1991).
10. M. Falk, in: *Chemistry and Physics of Aqueous Gas Solutions*, W. B. Adams et al. (eds.), Electrochem. Soc. Inc., Princeton (1975), pp. 19-41.
11. Yu. Ya. Efimov and Yu. I. Naberukhin, *J. Struct. Chem*., **41**, No. 3, 433-439 (2000).
12. H. Palamarev and G. Georgiev, *Mol. Struct*., **378**, 237-248 (1996).